Chemistry

(2*S*)-Di-*tert*-butyl 2-(3-(1-*tert*-butoxy)-1-oxo-6-(4-(tributylstannyl)benzamido)hexan-2-yl)ureido)pentanedioate (4). To a solution of 0.265 g (0.50 mmol) 6-(*tert*-butoxy)-5-3-((*S*)-1,5-di-*tert*-butoxy-1,5-dioxopentan-2-yl)ureido)-6-oxohexyl-1-ammonium formate (*1*) **2** dissolved in CH_2Cl_2 (5 mL) was added triethylamine (0.1 mL, 0.72 mmol), followed by *N*-succinimidyl-4-tributylstannylbenzoate (*2*) (0.30 g, 0.59 mmol). After stirring for 2 h at room temperature, the solvent was evaporated and the residue was purified on a silica column using MeOH/CH_2Cl_2 (5:95) to afford **4** (0.37 g, 84%). ^{1}H NMR (400 MHz, $CDCl_3$) δ 7.70 (d, J = 8.0 Hz, 2H), 7.50 (d, J = 8.0 Hz, 2H), 6.40 (m, 1H), 5.07-5.17 (m, 2H), 4.31 (m, 2H), 3.42 (m, 2H), 2.26-2.33 (m, 2H), 2.04-2.08 (m, 1H), 1.81-1.84 (m, 2H), 1.60-1.65 (m, 3H), 1.46-1.52 (m, 6H), 1.41-1.43 (m, 27H), 1.25-1.34 (m, 8H), 1.04-1.09 (m, 6H), 0.84-0.88 (m, 9H). ESI-Mass calcd. for $C_{43}H_{75}N_3O_8Sn$ M^+ 881.5, found 881.9.

Radiochemistry

Astatine was produced on a CS-30 cyclotron at Duke University and the NIH by bombarding natural bismuth metal targets with 28 MeV α-particles and isolated by dry distillation (*3, 4*). The ^{211}At was isolated in a solution of *N*-chlorosuccinimide (NCS) in MeOH (1 mg/mL).

Sodium [^{131}I]iodide in 0.1 N NaOH (44,400 GBq/mmol) was purchased from Perkin-Elmer. High performance liquid chromatography (HPLC) was performed on a Beckman Gold HPLC system (Beckman Coulter) equipped with a ScanRam RadioTLC scanner/HPLC γ-detector combination (LabLogic). A Waters XTerra C18, 4.6 × 250 mm, 5 µm was used for RP-HPLC.

(2*S*)-2-(3-(1-Carboxy-5-(4-[^{131}I]iodobenzamido)pentyl)ureido)pentanedioic acid ([^{131}I]5). This compound was prepared following the procedure for radiolabeling with ^{125}I using stannane **3** (Scheme 1) (*5*).

(2*S*)-2-(3-(1-Carboxy-5-(4-[^{211}At]asatatobenzamido)pentyl)ureido)pentanedioic acid ([^{211}At]6). A solution of ^{211}At in NCS/MeOH (74–370 MBq in 200-300 μL) and acetic acid (60 μL) was added to 50 μg of stannane precursor **3** or **4**. The reaction was allowed to proceed at 20°C for 10 min, the MeOH was evaporated under a gentle stream of argon, and a solution of anisole in TFA (3% v/v; 100 μL) was added to the residue. The reaction mixture was allowed to stand for 30 min at 50°C or 90 min at room temperature. The TFA was evaporated with argon and the compound reconstituted in 50 μL of 90:10 water:acetonitrile and injected onto a RP-HPLC column. The column was eluted at a flow rate of 1 mL/min with a gradient consisting of 0.1 % TFA in H_2O (solvent A) and 0.1 % TFA in acetonitrile (solvent B). Solvent B was kept at 5% for 5 min and then linearly increased to 100% over 30 min. Under those conditions, the product eluted with a t_R of ~20 min. HPLC fractions containing the radiolabeled product were pooled, and most of the acetonitrile was evaporated under a stream of argon. The resultant solution was diluted with water (10 mL) and passed through either an activated C18 Sep-Pak plus cartridge or an Oasis HLB Sep-Pak cartridge (Waters). The cartridge was washed with 10 mL of water and the product eluted with 0.25 mL portions of ethanol. The fractions containing most of the radioactivity (typically 2-5) were pooled, the ethanol was evaporated, and the product was reconstituted in PBS.

Dosimetry

The radioactivity concentration versus time curves were integrated using a hybrid numerical integration/analytical integration method to calculate the time-integrated activity. If the data could be fit to a mono-exponential expression, the curve was integrated analytically from zero to

infinity. Alternatively, numerical integration of the data and the last two time points was used to derive a mono-exponential function that was analytically integrated beyond the last measurement to infinity. The mean absorbed dose $D(r_T, T_D)$ to the whole kidney and tumor was calculated using the following expression:

$$D(r_T, T_D) = \tilde{A}(r_S, T_D) \cdot S(r_T \leftarrow r_T)$$

where $\tilde{A}(r_S, T_D)$ is the time-integrated activity and $S(r_T \leftarrow r_T)$ is the self absorbed dose per unit time-integrated activity (*6*). For ^{211}At $S(r_T \leftarrow r_T)$ = 1.088E-12 J/(Bq·s) (*7*), for the emitted α-particles, all energy emitted was assumed to be deposited within the kidney or tumor. For the β^--particles, a mouse-size kidney model (*8*) was used in GEANT4 Monte Carlo. Only the β^--particle energy was scored. The β^- ^{211}At $S(r_T \leftarrow r_T)$ was calculated to be 9.98E-16 J/(Bq·s) and was subsequently omitted.

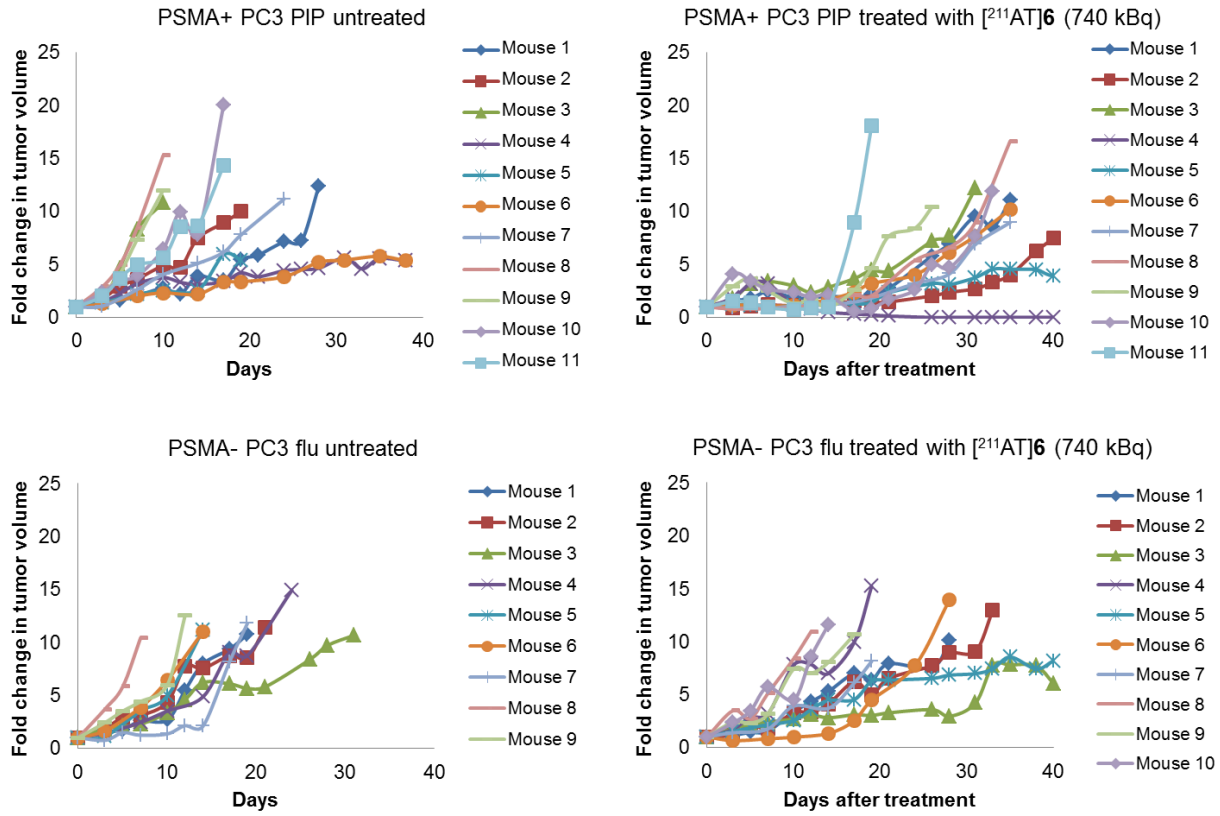

Supplemental Figure 1. Tumor volume changes upon treatment with 740 kBq (20 µCi) of [^{211}At]**6**. Each line represents one mouse. Mice with more than 10-fold tumor volume increase by the time of measurement were sacrificed.

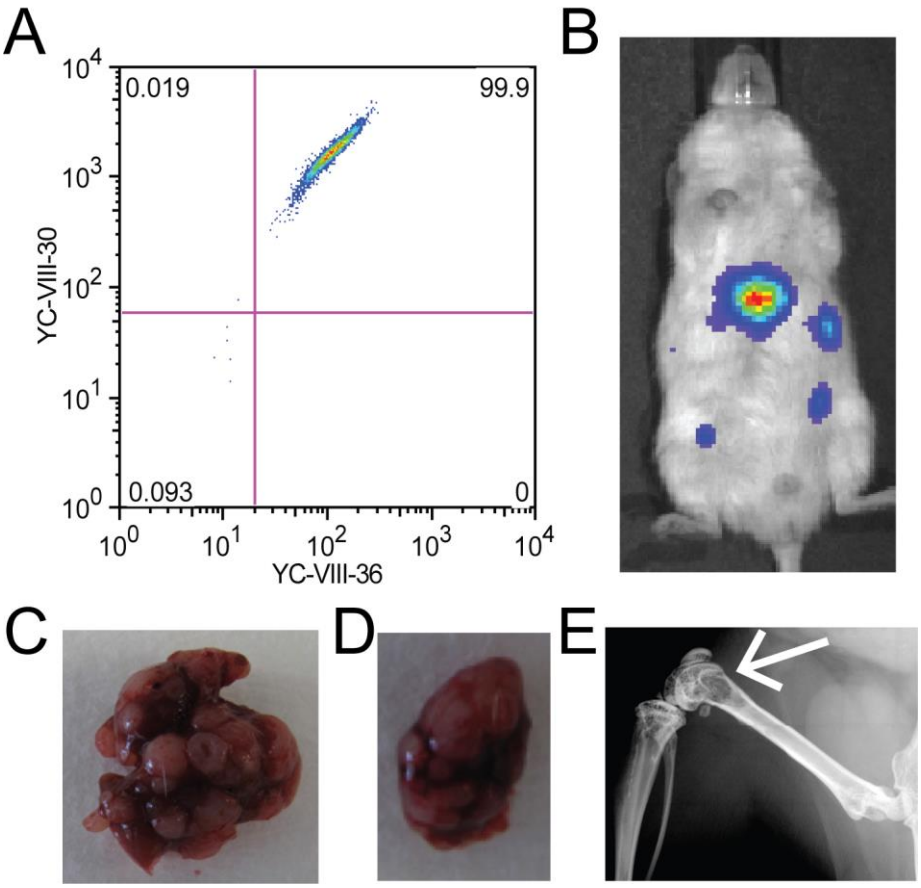

Supplemental Figure 2. Metastatic model of PSMA-expressing human prostate cancer. (A) FACS analysis using PSMA-targeted small molecules (YC-VIII-36 and YC-VIII-30 tagged with FITC and Bodipy, respectively). (B) Representative BLI image of a mouse injected with PC3-ML-Luc-PSMA. Metastatic lesions in liver (C) and kidney (D). (E) Digital X-ray showing lytic bone metastasis lesions in femur (arrow).

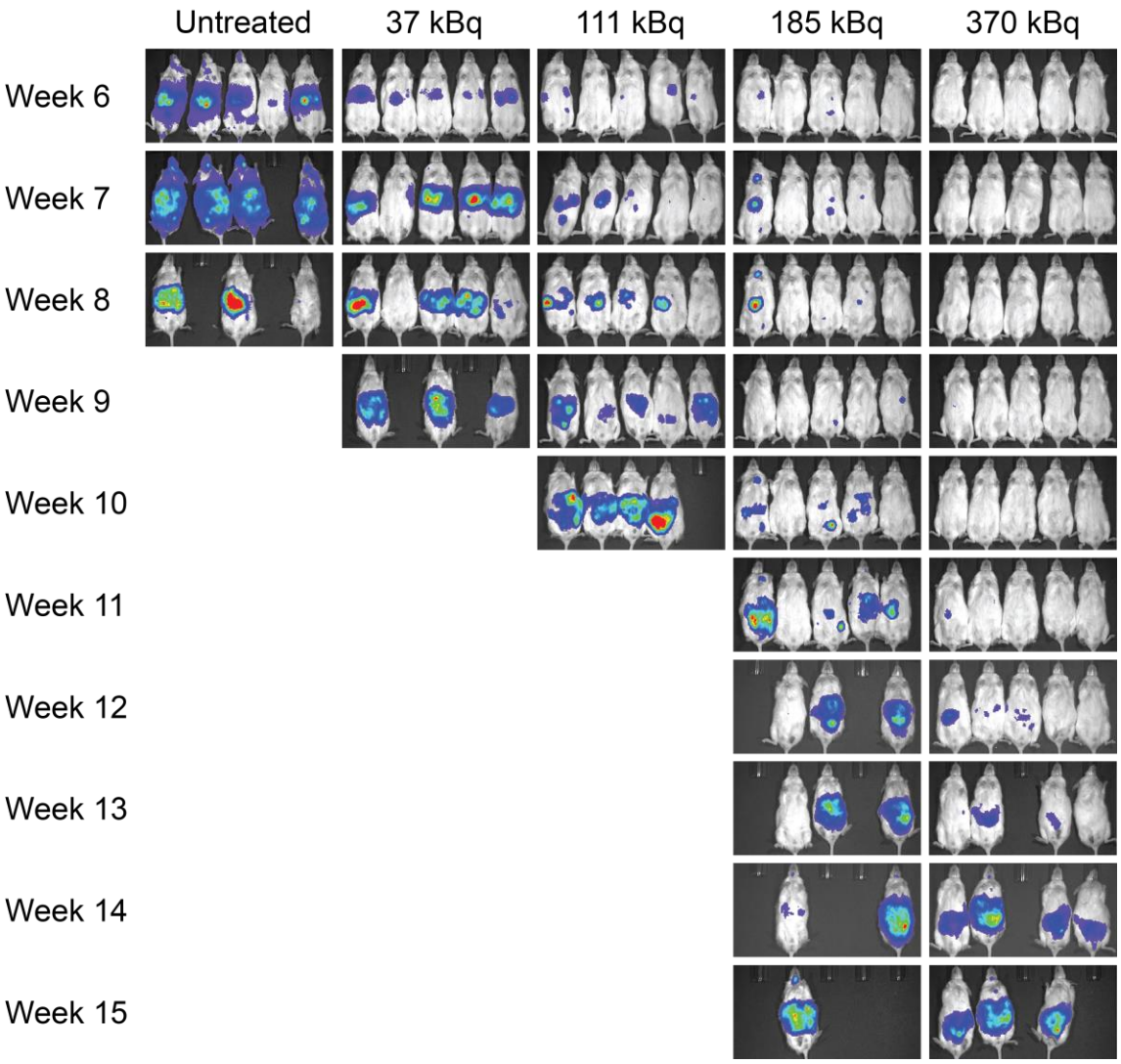

Supplemental Figure 3. [^{211}At]**6** showed significant tumor growth delay using the micrometastatic model. Bioluminescence images during the course of the treatment are shown.

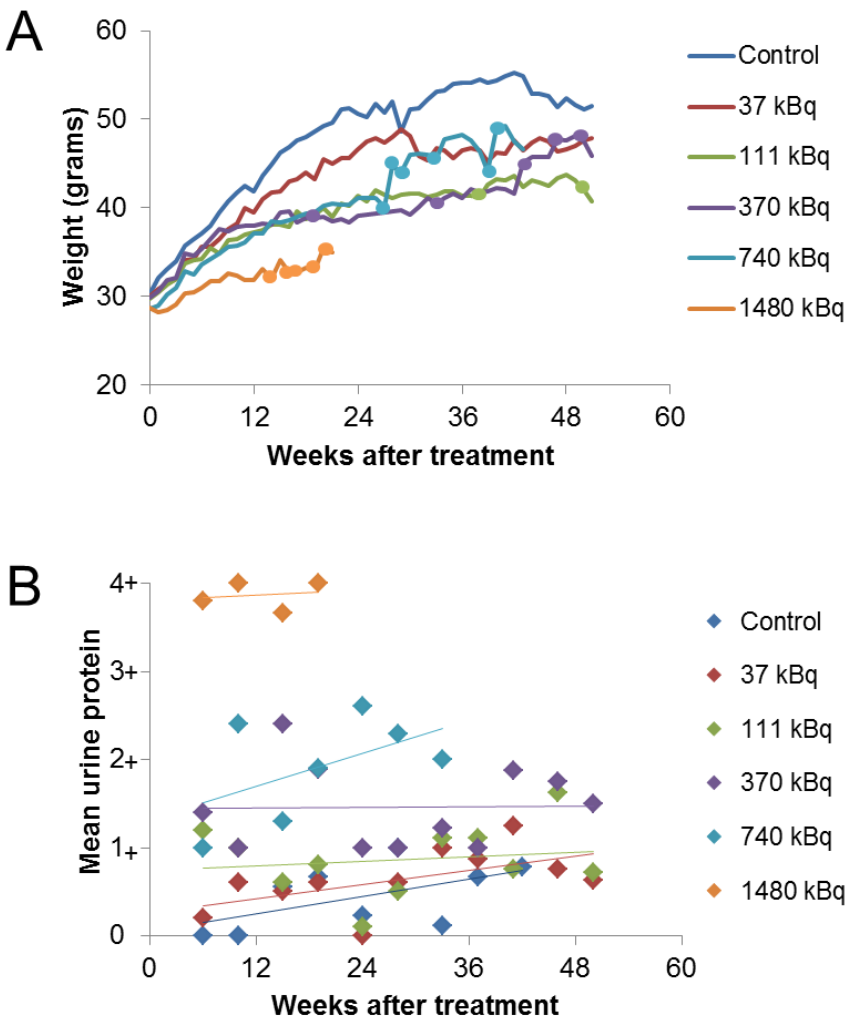

Supplemental Figure 4. (A) Weight and survival of CD1 mice after treatment with [^{211}At]**6**. The maximum tolerated dose was 37 kBq (1 µCi). Tick marks indicate times of animal death or sacrifice. (B) Urine protein level measured by dipstick showed dose-dependent proteinuria occurring several months before animal death in the higher dosage groups.

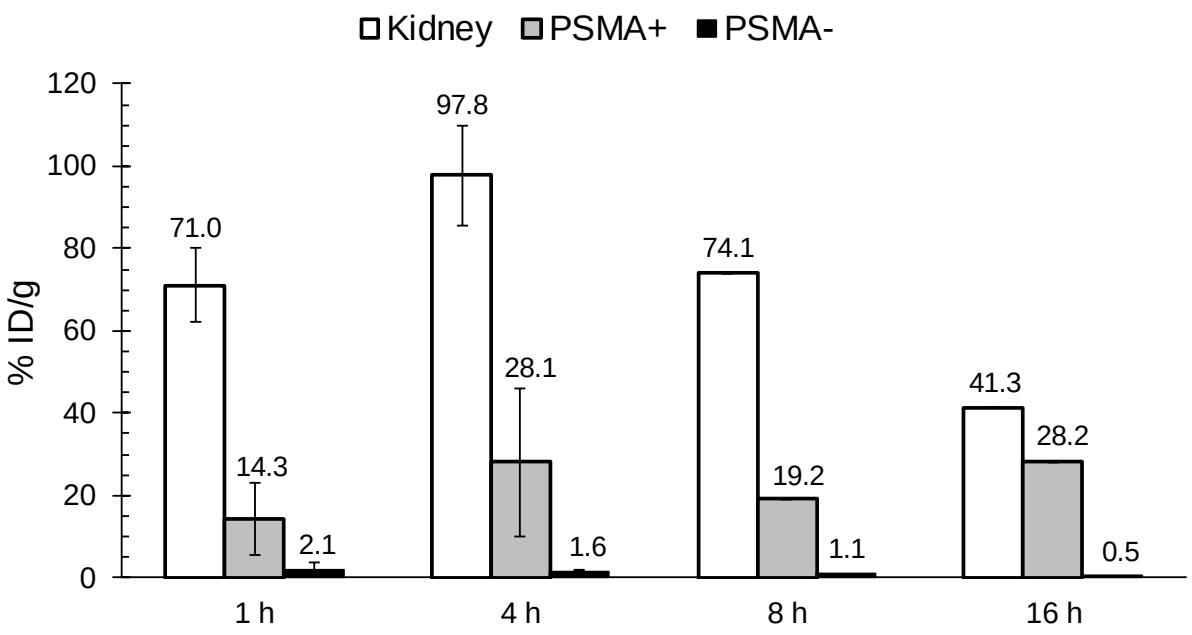

Supplemental Figure 5. Biodistribution of [^{211}At]**6** in kidney (white), PSMA+ PC3 PIP tumor (gray) and PSMA- PC3 flu tumor (black) at 1-16 h. Error bars are SD.

Supplemental Table 1. Paired-label biodistribution of [^{131}I]**5** and [^{211}At]**6** in athymic mice bearing PSMA+ PC3 PIP and PSMA- PC3 flu xenografts.

Iodine-131

Tissue	%Injected Dose/gram[a]				
	0.5 h	1 h	2 h	4 h	18 h
Liver	7.43 ± 1.92	5.56 ± 1.20	4.50 ± 0.44	3.77 ± 0.45	0.63 ± 0.14
Spleen	31.27 ± 6.41	36.13 ± 13.95	25.06 ± 6.80	25.18 ± 3.60	10.30 ± 1.99
Lung	4.28 ± 1.32	2.86 ± 2.32[c]	2.32 ± 0.82	2.22 ± 0.84	1.09 ± 0.20
Heart	1.87 ± 1.35	1.58 ± 0.44	0.88 ± 0.21	0.84 ± 0.39	0.41 ± 0.15
Kidney	95.17 ± 18.85	114.82 ± 16.10	100.38 ± 9.17	100.05 ± 20.06	119.42 ± 15.24
Stomach	0.90 ± 0.15	0.71 ± 0.24	0.55 ± 0.24	1.37 ± 1.07	0.406 ± 0.09
Sm. Intestine	2.12 ± 0.65	2.74 ± 0.54	1.88 ± 0.55[c]	1.62 ± 0.25[c]	0.42 ± 0.09
Lg. Intestine	0.64 ± 0.21	0.45 ± 0.09	2.58 ± 0.86[c]	3.89 ± 1.35[c]	0.71 ± 0.23
Thyroid[b]	0.01 ± 0.09	0.14 ± 0.06	0.03 ± 0.04	0.06 ± 0.04	0.04 ± 0.05
Muscle	0.95 ± 0.20[c]	0.69 ± 0.17	0.68 ± 0.18[c]	0.50 ± 0.13	0.40 ± 0.28[c]
Blood	1.30 ± 0.35	0.75 ± 0.24	0.37 ± 0.07	0.25 ± 0.04	0.07 ± 0.01
Bone	1.20 ± 0.15	1.11 ± 0.58	1.10 ± 1.01	1.20 ± 0.49	0.66 ± 0.35
Brain	0.10 ± 0.03	0.06 ± 0.02	0.05 ± 0.01	0.03 ± 0.00	0.02 ± 0.00

[a]Mean ± SD (n = 5); [b]%ID/organ; [c]Difference between the uptake of two isotopes non-significant.

Supplemental Table 2. Paired-label biodistribution of [^{131}I]**5** and [^{211}At]**6** in athymic mice bearing PSMA+ PC3 PIP and PSMA- PC3 flu xenografts.

Astatine-211

Tissue	%Injected Dose/gram[a]				
	0.5 h	1 h	2 h	4 h	18 h
Liver	3.16 ± 0.65	2.11 ± 0.65	1.58 ± 0.21	1.63 ± 0.10	0.82 ± 0.07
Spleen	27.72 ± 6.23	29.18 ± 10.20	20.30 ± 5.21	20.34 ± 3.55	8.01 ± 2.04
Lung	10.99 ± 2.72	5.82 ± 1.28[c]	6.30 ± 1.57	5.54 ± 1.79	3.61 ± 0.40
Heart	3.24 ± 0.63	2.36 ± 0.48	1.79 ± 0.31	1.65 ± 0.39	1.10 ± 0.16
Kidney	68.01 ± 11.99	71.53 ± 11.86	60.16 ± 6.16	60.19 ± 57.37	57.37 ± 7.36
Stomach	7.19 ± 1.96	10.09 ± 1.66	9.29 ± 2.86	13.32 ± 3.12	9.42 ± 3.04
Sm. Intestine	3.94 ± 0.87	3.67 ± 0.65	2.08 ± 0.41[c]	1.85 ± 0.23[c]	1.08 ± 0.10
Lg. Intestine	1.37 ± 0.39	1.12 ± 0.21	2.78 ± 0.21[c]	2.39 ± 0.33[c]	0.99 ± 0.21
Thyroid[b]	0.46 ± 0.13	0.79 ± 0.33	0.62 ± 0.23	0.54 ± 0.22	1.32 ± 0.62
Muscle	1.23 ± 0.42[c]	0.95 ± 0.15	0.81 ± 0.12[c]	0.72 ± 0.14	0.49 ± 0.27[c]
Blood	2.51 ± 0.52	1.67 ± 0.32	1.26 ± 0.15	0.99 ± 0.12	0.53 ± 0.05
Bone	1.92 ± 0.41	1.78± 0.48	1.64 ± 1.07	1.65 ± 0.49	1.03 ± 0.35
Brain	0.40 ± 0.10	0.27 ± 0.08	0.25 ± 0.05	0.20± 0.02	0.11 ± 0.02

[a]Mean ± SD (n = 5); [b]%ID/organ; [c]Difference between the uptake of two isotopes non-significant.

REFERENCES

1. Maresca KP, Hillier SM, Femia FJ, et al. A series of halogenated heterodimeric inhibitors of prostate specific membrane antigen (PSMA) as radiolabeled probes for targeting prostate cancer. *Journal of medicinal chemistry.* Jan 22 2009;52(2):347-357.

2. Dekker B, Keen H, Shaw D, et al. Functional comparison of annexin V analogues labeled indirectly and directly with iodine-124. *Nuclear medicine and biology.* May 2005;32(4):403-413.

3. Pozzi OR, Zalutsky MR. Radiopharmaceutical chemistry of targeted radiotherapeutics, Part 3: alpha-particle-induced radiolytic effects on the chemical behavior of (211)At. *Journal of nuclear medicine : official publication, Society of Nuclear Medicine.* Jul 2007;48(7):1190-1196.

4. Schwarz UP, Plascjak P, Beitzel MP, Gansow OA, Eckelman WC, Waldmann TA. Preparation of 211At-labeled humanized anti-Tac using 211At produced in disposable internal and external bismuth targets. *Nuclear medicine and biology.* Feb 1998;25(2):89-93.

5. Chen Y, Foss CA, Byun Y, et al. Radiohalogenated prostate-specific membrane antigen (PSMA)-based ureas as imaging agents for prostate cancer. *Journal of medicinal chemistry.* Dec 25 2008;51(24):7933-7943.

6. Bolch WE, Eckerman KF, Sgouros G, Thomas SR. MIRD pamphlet No. 21: a generalized schema for radiopharmaceutical dosimetry--standardization of nomenclature. *Journal of nuclear medicine : official publication, Society of Nuclear Medicine.* Mar 2009;50(3):477-484.

7. Loevinger R, T.F. B, Watson EE. MIRD Primer for Absorbed Dose Calculations. New York, NY: The Society of Nuclear Medicine, Inc.; 1991.

8. Bouchet LG, Bolch WE, Blanco HP, et al. MIRD Pamphlet No 19: absorbed fractions and radionuclide S values for six age-dependent multiregion models of the kidney. *Journal of nuclear medicine : official publication, Society of Nuclear Medicine.* Jul 2003;44(7):1113-1147.